Density functional theory for solids

International summer School in electronic structure Theory: electron correlation in Physics and Chemistry

Centre Paul Langevin, Aussois, Savoie, France

Xavier Blase

Institut Néel, CNRS, Grenoble, France.

June 11, 2015

Introduction

The title "DFT for solids" does not mean that there is some specific density functional theory for solids: DFT remains DFT (see lectures by Prof. Julien Toulouse) but there are just specific implementations (e.g. planewaves), specific difficulties (defects, charged systems, incommensurate perturbations or instabilities, etc.) and specific ways of thinking about the exchange-correlation functional (short versus long-range screening in metals or insulators).
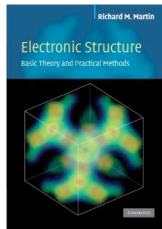
Book: Electronic Structure: Basic Theory and Practical Methods, Richard M. Martin, Cambridge University Press (2008).

Real systems are usually inhomogeneous

IV. CONCLUDING REMARKS

In the preceding sections we have developed a theory of the electronic ground state which is exact in two limiting cases: The case of a nearly constant density $(n = n_0 + \bar{n}(r), \bar{n}(r)/n_0 \ll 1)$ and the case of a slowly varying density. Actual electronic systems do not belong to either of these two categories. The most promising formulation of the theory at present appears to be that obtained by partial summation of the gradient expansion (Sec. III.4). It has, however, not yet been tested in actual physical problems.

In atoms and molecules one can distinguish three regions: (1) A region near the atomic nucleus, where the electronic density is high and therefore, in view of case (b) above, we expect our procedure to be satisfactory. (2) The main "body" of the charge distribution where the electronic density $n(\mathbf{r})$ is relatively slowly varying, so that our approximation (2.3) for ϵ_{xc} is expected to be satisfactory as discussed in case (a) above. (3) The "surface" of atoms and the overlap regions in molecules. Here our approximation (2.3) has no validity and therefore we expect this region to be the main source of error. We do not expect an accurate description of chemical binding.

High density limit: kinetic energy dominates
Approximation (2.3) = local density approximation
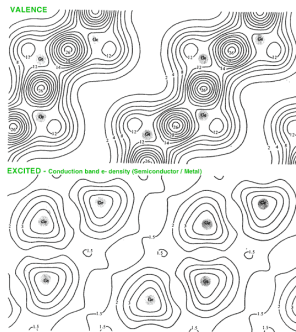
Plot of the charge density $|\psi_{n\mathbf{k}}|^2$ associated with the top of the valence bands and bottom of the conduction bands in Germanium, a "nearly" metal (courtesy Prof. Majewsky, Virginia U.)

Real systems are not in the low or high density limit

Standard extended condensed-matter or solid-state-physics systems are difficult since they are not in a limit where standard perturbation theory starting from the high or low-density limits can work "accurately".
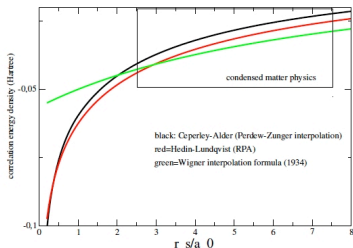
Correlation energy density for the interacting electron gas as a function of the Wigner-Seitz radius (r_S) which is the radius of the gedanken sphere whose volume is the total volume divided by the number of electrons ($\Omega_{WS} = 4\pi r_S^3/2 = \Omega/N$).

Analytic low-density (Wigner limit where potential energy dominates) and high-density (RPA limit where kinetic energy dominates) are compared to "exact" numerical Quantum Monte Carlo data by Ceperley and Alder (D.M. Ceperley and B.J. Alder, PRL 1980).

DFT/LDA charge density in inhomogeneous systems

As shown here for solid argon, with very inhomogeneous charge densies, the DFT/LDA charge density is in excellent agreement with higher level approaches [PRB 74, 045102 (2006)].
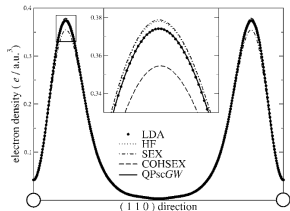
FIG. 7. Argon: density along the direction (1 1 0) within different approximations. The inset is a close-up of the region around the maximum.

LDA
HF
SEX
COHSEX
QPscGW

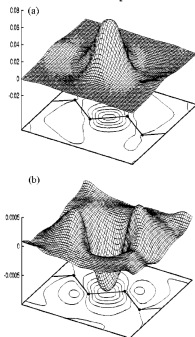electron density (e / a.u.^{3})

(1 1 0) direction

FIG. 2. (a) The VMC one-body density matrix, $\rho_{VMC}(\mathbf{r}, \mathbf{r}')$ and (b) $\rho_{VMC}(\mathbf{r}, \mathbf{r}') - \rho_{LDA}(\mathbf{r}, \mathbf{r}')$, in the (110) plane passing through the atoms with $\mathbf{r}$ fixed at the bond center. ρ is normalized such that $\rho(\mathbf{r}, \mathbf{r}) = n(\mathbf{r})$, the charge density at the bond center. The silicon atoms and bonds are shown schematically.

$$\rho_{VMC}(\mathbf{r}, \mathbf{r}') = N \int \psi^*(\mathbf{r}, \mathbf{r}_2, ..., \mathbf{r}_N)\psi(\mathbf{r}', \mathbf{r}_2, ..., \mathbf{r}_N) \, d\mathbf{r}_2...d\mathbf{r}_N$$

$$\rho_{LDA}(\mathbf{r}, \mathbf{r}') = \sum_n \phi_i^*(\mathbf{r})\phi_i(\mathbf{r}')\theta(E_F - \varepsilon_n)$$

Spherically averaged XC hole and the associated sum rule

The success of DFT/LDA even for highly inhomogeneous systems can be related to the quality of the "spherically averaged" exchange-correlation hole and the fact that the LDA XC-hole satisfies the correct sum-rule.

$$E^{XC} = \frac{1}{2} \int d\mathbf{r}_1 d\mathbf{r}_2 \frac{\rho(\mathbf{r}_1)\rho_{xc}(\mathbf{r}_1, \mathbf{r}_2)}{|\mathbf{r}_2 - \mathbf{r}_1|} \quad \text{and} \quad \int d\mathbf{r}_2 \, \rho_{xc}(\mathbf{r}_1, \mathbf{r}_2) = -1.$$
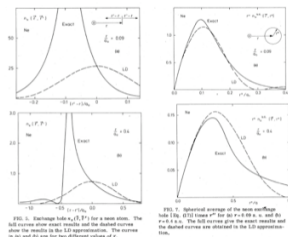
Exact versus LDA exchange hole for Neon atom along specific directions (left) and spherically averaged (right). (Gunnarsson et al. PRB 1979)
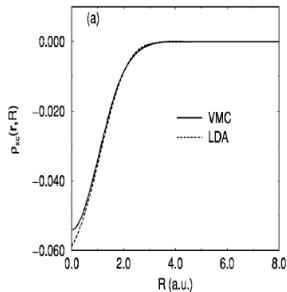
Exact (VMC) versus LDA spherically averaged XC-hole for silicon. [PRB 57, 15293 (1998)]

Minimal reminder: the total energy

The total energy of the system reads (atomic units: $4\pi\epsilon_0 = e = \hbar = 1$):

$$E_0 = \sum_n^{occp} <\phi_n|\frac{-\nabla^2}{2}|\phi_n> + \int d\mathbf{r}\ V^{ion}(\mathbf{r})n(\mathbf{r}) + \frac{1}{2}\int\int \frac{n(\mathbf{r})n(\mathbf{r}')}{|\mathbf{r}-\mathbf{r}'|}$$
$$+ E^{XC}[n] + \frac{1}{2}\sum_{IJ}\frac{Z_I Z_J}{|\tau_I - \tau_J|} \quad \text{with} \quad V^{ion}(\mathbf{r}) = \sum_J \frac{-Z_J}{|\tau_J - \mathbf{r}|},$$

with (Z_J, τ_J) the charge and position of the ions and $E^{XC}[n]$ the exchange-correlation energy. We recognise the kinetic energy (really $T - T_0 + E^{ee} - J$), the ionic (external) potential, the Hartree (classical) energy, the exchange and correlation energy and the ion-ion Coulomb interaction.

> The total energy should be that of the ... unit cell !!

If you double your unit cell, you should obtain an energy twice as large.

Minimal reminder: the Kohn-Sham equation

The Kohn-sham equation, namely the effective one-body eigenvalue equation, reads:

$$\left(\frac{-\nabla_{\mathbf{r}}^2}{2} + V^{eff}(\mathbf{r})\right)\phi_n(\mathbf{r}) = \varepsilon_n\phi_n(\mathbf{r})$$

with $V^{eff}(\mathbf{r}) = V^{ion}(\mathbf{r}) + V^H(\mathbf{r}) + V^{XC}(\mathbf{r})$, and:

- $V^{ion}(\mathbf{r}) = \sum_J(-Z_J)/|\tau_J - \mathbf{r}|$ the ionic (external) potential,
- $V^H(\mathbf{r}) = \int d\mathbf{r}' n(\mathbf{r}')/|\mathbf{r} - \mathbf{r}'|$ the Hartree potential,
- $V^{XC}(\mathbf{r}) = \partial E^{XC}[n]/\partial n(\mathbf{r})$ the exchange-correlation potential.

with (Z_J, τ_J) the charge and position of the ions and $E^{XC}[n]$ the exchange-correlation energy. We use atomic units, namely $4\pi\epsilon_0 = e = \hbar = 1$.

Minimal reminder: second formulation of total energy

We can also observe:

$$\sum_n^{occp} \varepsilon_n = \sum_n^{occp} < \phi_n | \hat{H} | \phi_n > = \sum_n^{occp} < \phi_n | \frac{-\nabla^2}{2} | \phi_n >$$
$$+ \int d\mathbf{r} \; n(\mathbf{r}) \; \left(V^{ion}(\mathbf{r}) + V^H(\mathbf{r}) + V^{XC}(\mathbf{r}) \right),$$

with: $\sum_n^{occp} |\phi_n(\mathbf{r})|^2 = n(\mathbf{r})$, so that the total energy reads:

$$E_0 = \sum_n^{occp} \varepsilon_n - \frac{1}{2} \int \int \frac{n(\mathbf{r})n(\mathbf{r}')}{|\mathbf{r} - \mathbf{r}'|} + E^{XC} - \int d\mathbf{r} \; n(\mathbf{r}) V^{XC}(\mathbf{r})$$

with: $V^{XC}(\mathbf{r}) = \partial E^{XC} / \partial n(\mathbf{r})$.

The plane wave formalism

The planewave formalism, namely the use of planewaves (PWs) as a basis, is certainly the most widespread technique in codes dedicated to deal with solids and periodic boundary conditions. In the field of solid-state physics, it comes however after other pioneering approaches such as the muffin-tin approach (total energy calculations by DeCicco et al. in 1965) where the space was paved with non-overlapping spheres and a spherical basis was adopted within the spheres, opening the way to the modern FLAPW techniques.

Planewaves offer a more systematic and unbiased way of describing the variations of the wavefunctions, density, potentials, etc. in space. Further, planewaves are very naturally associated with the Bloch theorem and the Fourier series we have seen for a periodic object.

A standard original article for learning in more details the PWs formalism combined with DFT is: "Momentum-space formalism for the total energy of solids", J. Ihm, Alex Zunger and Marvin L Cohen, J. Phys. C: Solid State Phys., Vol. 12, 1979.

The Fourier transform properties

Fourier transform a periodic function, with Ω the crystal volume and $\{\mathbf{G}\}$ the reciprocal lattice vectors:

$$f(\mathbf{r}) = \sum_{\mathbf{G}} f(\mathbf{G})e^{i\mathbf{G}\cdot\mathbf{r}} \quad \text{and} \quad f(\mathbf{G}) = \frac{1}{\Omega}\int f(\mathbf{r})e^{-i\mathbf{G}\cdot\mathbf{r}}d\mathbf{r}$$

Several important properties can be exploited:

- plane waves are orthogonal: $\int e^{i(\mathbf{G}-\mathbf{G}')\cdot\mathbf{r}}d\mathbf{r} = \Omega\delta(\mathbf{G},\mathbf{G}')$
- the Fourier transform of a convolution product is a direct product:

$$\frac{1}{\Omega}\int d\mathbf{r}e^{-i\mathbf{G}\cdot\mathbf{r}}\int d\mathbf{r}'\, f(\mathbf{r}')g(\mathbf{r}-\mathbf{r}') = \Omega f(\mathbf{G})g(\mathbf{G})$$

- Parseval's relation (f and g have the lattice periodicity):

$$\int f(\mathbf{r})g(\mathbf{r})\frac{d\mathbf{r}}{\Omega} = \sum_{\mathbf{G}} f(-\mathbf{G})g(\mathbf{G}) \quad \text{or} \quad \int f^*(\mathbf{r})g(\mathbf{r})\frac{d\mathbf{r}}{\Omega} = \sum_{\mathbf{G}} f(\mathbf{G})g(\mathbf{G})$$

Representation of the density and Hartree potential

We now exploit Poisson's equation (in atomic units: $4\pi\epsilon_0 = 1$):

$$V_H(\mathbf{r}) = \int \frac{n(\mathbf{r}')\,d\mathbf{r}'}{|\mathbf{r} - \mathbf{r}'|} \quad and \quad \nabla^2 V_H(\mathbf{r}) = -4\pi n(\mathbf{r}),$$

which by Fourier transform :

$$|\mathbf{G}|^2 V_H(\mathbf{G}) = -4\pi n(\mathbf{G}) \quad \Rightarrow \quad V_H(\mathbf{G}) = \frac{4\pi n(\mathbf{G})}{|\mathbf{G}|^2}.$$

The Hartree energy per cell then reads (N number of unit cells):

$$\frac{1}{2N} \int d\mathbf{r}\, n(\mathbf{r}) V^H(\mathbf{r}) = \frac{\Omega}{2N} \sum_{\mathbf{G}} n(-\mathbf{G}) V_H(\mathbf{G}) = 2\pi\Omega_{cell} \sum_{\mathbf{G}} \frac{n(-\mathbf{G})n(\mathbf{G})}{|\mathbf{G}|^2}.$$

In the planewave formalism, no need for the four-centre two-electrons integrals as encountered in Gaussian-basis codes.

Planewave cutoff

We cannot use an infinite planewave basis (there is an infinite number of $e^{i\vec{G}\cdot\vec{r}}$). Assume you want to describe wavefunctions on a real-space grid with a (dx=dy=dz) spacing between your grid points. Then you need to include planewaves that offer a variation on that lengthscale, namely qualitatively: $\lambda_{min} \leq dx \Rightarrow G_{max} \geq 2\pi/dx$.

Planewave expansion: $u_{n\mathbf{k}}(\mathbf{r}) = \sum_{\mathbf{g}} c_{n\mathbf{k}}(\mathbf{G})e^{i\vec{G}\cdot\vec{r}}$

with: $\frac{1}{2}|\mathbf{k} + \mathbf{G}|^2 \leq E_{cut}^{max}$

The size of your planewave basis is the number of reciprocal vectors $\mathbf{G}$ within the sphere in reciprocal space of radius G_{max} such that the cut-off criteria on the planewave kinetic-energy is fulfilled.

Courtesy Xavier Gonze
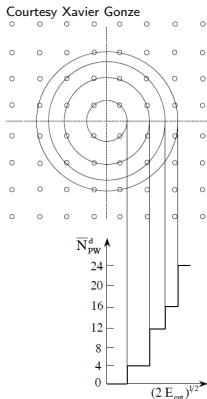
Representation of the density and the two energy cutoffs

The density contributed by one occupied Kohn-Sham state: $\phi_{n\mathbf{k}} = e^{i\mathbf{k}\cdot\mathbf{r}}u_{n\mathbf{k}}(\mathbf{r})$, where $u_{n\mathbf{k}}(\mathbf{r})$ is periodic, reads:

$$\rho_{n\mathbf{k}}(\mathbf{r}) = |\phi_{n\mathbf{k}}(\mathbf{r})|^2 = |u_{n\mathbf{k}}(\mathbf{r})|^2 \quad \text{with} \quad u_{n\mathbf{k}}(\mathbf{r}) = \sum_{\mathbf{G}} u_{n\mathbf{k}}(\mathbf{G})e^{i\vec{G}\cdot\vec{r}}$$

The Fourier transform yields: $\rho_{n\mathbf{k}}(\mathbf{r}) = \sum_{\mathbf{G}\mathbf{G}'} u^*_{n\mathbf{k}}(\mathbf{G})u_{n\mathbf{k}}(\mathbf{G}')e^{i(\vec{G}'-\vec{G})\cdot\vec{r}}$

If the wavefunctions have nonzero coefficients for $\mathbf{G}$-vectors such that $|\mathbf{k} + \mathbf{G}|^2/2 < E_{cut}$, then the charge density as components up to $4E_{cut}$.

In principles, E_{cut} is the only parameter. In practice, one can always plays with a second cutoffs on the charge density.
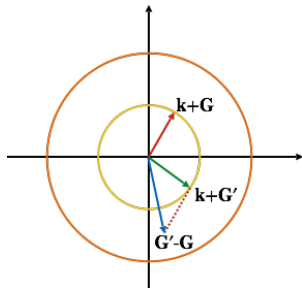
From real-space to reciprocal space

A important technique is the fast Fourier transform (FFT) which scales as O(NlogN) !!!

Since most exchange-correlation functional are a function of the charge density $\rho(\mathbf{r})$ in real-space, one usually performs FFT back and forth:
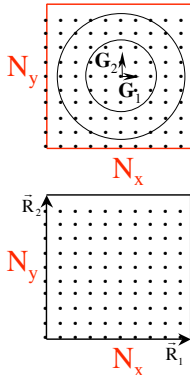
$$\rho(\mathbf{G}) \Rightarrow \rho(\mathbf{r}) \Rightarrow V^{xc}(\rho(\mathbf{r})) \Rightarrow V^{xc}(\mathbf{G})$$

or for the XC-energy density per particle:

$$\rho(\mathbf{G}) \Rightarrow \rho(\mathbf{r}) \Rightarrow \epsilon^{xc}(\rho(\mathbf{r})) \Rightarrow \epsilon^{xc}(\mathbf{G})$$

and the exchange-correlation energy per cell reads:

$E^{XC}/N = \int \frac{d\mathbf{r}}{N} n(\mathbf{r}) \epsilon^{xc}(\mathbf{r}) = \Omega_{cell} \sum_{\mathbf{G}} n(-\mathbf{G}) \epsilon^{xc}(\mathbf{G}).$

The external (ionic) potential

Assume (sp=1,N_{sp}) species and ($\sum_{sp} n_{sp}$) atoms in the unit-cell with position $\tau_{sp,j}$ ($j = 1, n_{sp}$). The ionic potential reads:

$$V^{ion}(\mathbf{r}) = \sum_{sp=1}^{N_{sp}} \sum_{j=1}^{n_{sp}} \sum_{\mathbf{R}} V_{at}^{sp}(\mathbf{r} - \tau_{sp,j} - \mathbf{R}),$$

where $V_{at}^{sp}(\mathbf{r})$ is the atomic potential for species (sp). Then:

$$V^{ion}(\mathbf{G}) = \int \frac{d\mathbf{r}}{\Omega} V^{ion}(\mathbf{r}) e^{-i\mathbf{G}\cdot\mathbf{r}} = \sum_{sp=1}^{N_{sp}} \int d\mathbf{u} V_{at}^{sp}(\mathbf{u}) e^{-i\mathbf{G}\cdot\mathbf{u}} \sum_{j=1}^{n_{sp}} e^{-i\mathbf{G}\cdot\tau_{sp,j}}$$

$$\left(\times \sum_{\mathbf{R}} \frac{e^{-i\mathbf{G}\cdot\mathbf{R}}}{\Omega} \right) = \frac{1}{\Omega_{cell}} \sum_{sp=1}^{N_{sp}} V_{at}^{sp}(\mathbf{G}) S^{sp}(\mathbf{G})$$

where $V_{at}^{sp}(\mathbf{G})$ and $S^{sp}(\mathbf{G})$ are the Fourier components of the atomic potential and structure factor for species (sp).
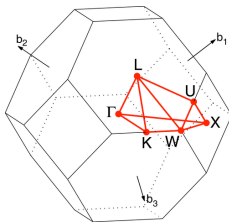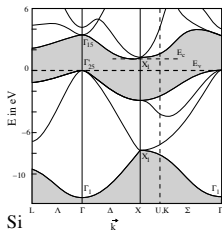
The kinetic energy and the Brillouin zone sampling

We have calculated all terms, besides the kinetic energy of the Kohn-Sham states, or, alternatively, the band energy contribution:

$$T_0 = \sum_n^{occp} < \phi_n | \frac{-\nabla^2}{2} | \phi_n > \quad \text{or} \quad E_{band} = \sum_n^{occp} \varepsilon_n$$

But really in a solid: $\sum_n^{occp} \Rightarrow \sum_{n\mathbf{k}}^{BZ,occp} \Rightarrow$ we have to sum over all **k**-points in the Brillouin zone (BZ) and over all occupied bands for a given **k**-point.
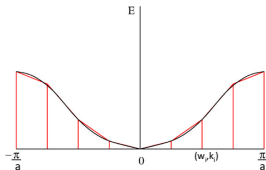

FCC path: Γ-X-W-K-Γ-L-U-W-L-K|U-X

[Setyawan & Curtarolo, DOI: 10.1016/j.commatsci.2010.05.010]

Brillouin zone sampling

Reminder: let's assume a chain of N-atoms with spacing (a). The BZ contains N k-points between $(-\pi/a)$ and (π/a) spaced by $(2\pi/Na)$. Assume you want to calculate the kinetic energy or band energy per cell. Then you must integrate over the states in the BZ.


We need a discrete sampling:

$$\frac{1}{N} \int_{-\pi/a}^{\pi/a} \frac{dk}{(2\pi/Na)} \simeq \sum_i w_i \delta(k - k_i).$$

But: $\frac{1}{N} \int_{-\pi/a}^{\pi/a} \frac{dk}{(2\pi/Na)} = 1.$

where the (1/N) is used to get a quantity (energy, etc.) per cell. The BZ can thus be sampled by a set of **k**-points mapping the Brillouin zone (BZ) such that $\sum_k w_k = 1$.

Brillouin zone sampling (II)

We sample the Brillouin zone with a set of **k**-points and calculate the Kohn-Sham eigenvalues for such **k**-points. How well our set of **k**-points samples the BZ is a convergency parameter: one should slowly increase the density of **k**-points in the BZ until convergency is reached !
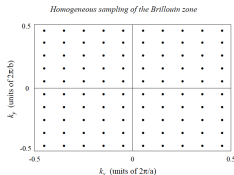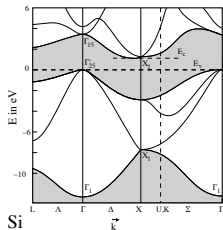
Band energy per unit cell:

$$\sum_{n\mathbf{k}} w_{\mathbf{k}} \varepsilon_{n\mathbf{k}} \theta(E_F - \varepsilon_{n\mathbf{k}})$$

with: $\sum_{n\mathbf{k}} w_{\mathbf{k}} = 1$.

Similarly: $n(\mathbf{r}) = \sum_{n\mathbf{k}} w_{\mathbf{k}} |\phi_{n\mathbf{k}}(\mathbf{r})|^2 \theta(E_F - \varepsilon_{n\mathbf{k}})$.

As a matter of fact, standard efficient grids are regular grids sampling the BZ: a (8x8x8)-grids separate the BZ in 8^3 little cubes ($\mathbf{b}_1/8, \mathbf{b}_2/8, \mathbf{b}_3/8$).

See e.g.: H. J. Monkhorst and J. D. Pack, Phys.Rev B13, 5188(1976).

A standard convergency test

We can now calculate the total energy (per cell) of solids. We need to increase the basis size and **k**-point sampling grid to reach convergency. For the convergency with planewaves, we decide of a maximum kinetic energy and take all **G**-vector components such that:

$$\frac{1}{2}|\mathbf{k} + \mathbf{G}|^2 \leq E_{cut} \Rightarrow \text{ FFT grid spacing } dx = 2\pi/G_{max}.$$

Convergence with E_{cut} (Si8)
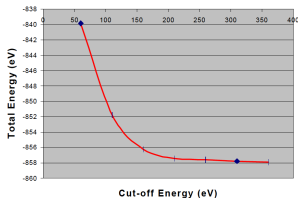
The real-space scale $dx = 2\pi/G_{max}$ should be smaller than the typical scale variations of the charge density. One can see why PWs do not like core states: very many PWs required to describe a localized object.

The BZ sampling is related to the complexity of the band-structure and the topology of the Fermi surface (gap or not, bands crossing, etc.)

Last "technical" issue: The pseudoptential approximation

Pseudopotentials in solids are of the same nature than pseudopotentials in e.g. Gaussian-basis codes: they remove core electrons, reducing the number of degree of freedoms. But there is another crucial goal which is to smooth out the oscillations of valence orbitals in the core regions: by orthogonality with core states, valence orbitals must vary rapidly in the core regions. Such oscillations cost literally thousands of planewaves !!! The wording "soft, "ultra-soft" refer to the smoothness of the generated pseudopotential.
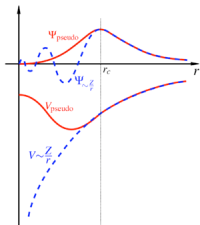
Figure. In dashed blue, the all-electron (ae) wavefunction, with oscillations in the core region, and the ($-Z/r$) ionic Coulomb potential. In red, the "pseudized" (ps) wavefunctions and ionic potential with smooth behavior. All-electron and "pseudized" quantities overlap beyond the core radius r_C. The pseudopotential is designed such that its action on the pseudo-wavefunction provide the "true" all-electron (Kohn-Sham) eigenvalue:

$$\left(\frac{-\nabla^2}{2} + \hat{V}_{ps}^{ion} + \hat{V}^{HXC} \right) \phi_{ps}^{at}(\mathbf{r}) = \varepsilon_{ae}^{at} \phi_{ps}^{at}(\mathbf{r})$$

Determination of the unit cell
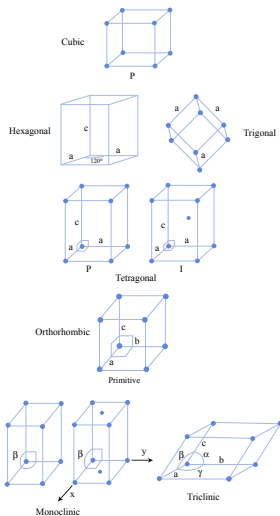
The first step is to determine the crystal structure, namely the Bravais lattice to which the solid belongs. In the case of the triclinic systems, the length of the lattice vectors $(\vec{a}_1, \vec{a}_1, \vec{a}_1)$ (noted $\vec{a}, \vec{b}, \vec{c}$ in the figure) and the angles between these vectors: α, β, γ, needs to be found by minimising the energy: $E = E(\vec{a}_1, \vec{a}_2, \vec{a}_3)$.

For each set of lattice vectors, the position of the atoms in the unit-cell must be determined $\Rightarrow$ inner loop of energy minimisation to get the position of atoms at equilibrium in the unit cell.
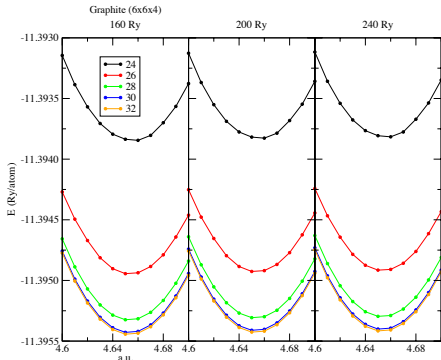$E = E_{(\vec{a}_1, \vec{a}_2, \vec{a}_3)}(\{\tau_i\})$, with $\{\tau_i\}$ the position of the atoms in the unit cell.

Lattice parameter and convergency

Graphite is hexagonal: needs to calculate in plane lattice parameter ($a = \sqrt{3}d_{CC}$) and (c) which is twice the interplant distance in the AB stacking. $a_{exp} = \sqrt{3} \times 1.42\ \mathring{A} = 4.65\ a.u.$
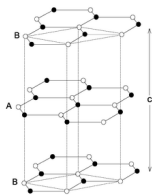

- Total energy of graphite, 6x6x4 k-point grid, ecutwfc=24, 26, 28, 30, 32 ; ecutrho = 160, 200, 240

Convergency tests for graphite: energy versus lattice parameter for various wave functions and density plane wave energy cutoffs (courtesy: Nicola Marzari, Quantum Espresso Pseudopotential webpages).

Pulay's errors and basis size finiteness

- Total energy of diamond, 4x4x4 k-point grid, ecutwfc=24, 26, 28, 30, 32 ; ecutrho = 160, 200, 240
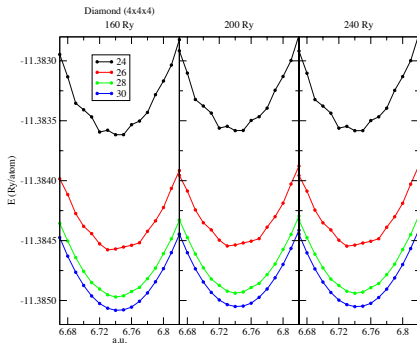
At low cutoff, one can see a weird behavior in the variations of the energy with respect to the lattice parameter. This is an effect of the non-completness and "granularity" of the **G**-vector basis that show at small energy cutoff.
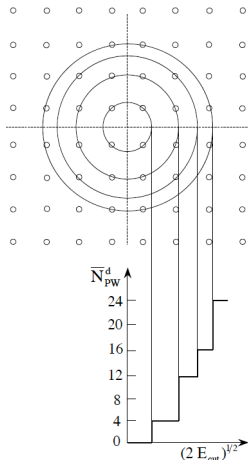
(Courtesy Xavier Gonze/Gian-Marco Rignanese)

Pulay's errors and basis size finiteness (II)

Upon changing the lattice vectors, the spacing between the **G**-vectors changes so that their number within the sphere of radius G_{max} changes: we do not treat cells with different volumes on the same footing !!
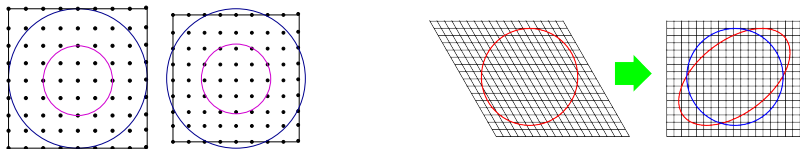
Figure: (Left) Changes in the reciprocal lattice upon volume cell change: the two circles are the fixed wavefunction and density energy cutoffs. (Right) Same physics in the case of a deformation of the unit cell shape involved in searching the equilibrium crystal structure.

Cure: increase energy cutoff or apply "corrections". See e.g. G P Francis and M C Payne, J. Phys.: Condens. Matter 2 (1990) 4395-4404.

What is the unit cell ?
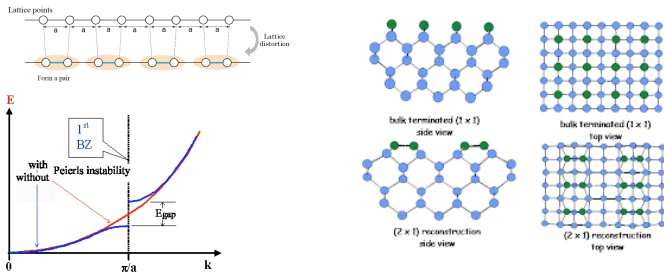
Do we really have the correct structure ? We did our best but within the hard constraint of the number of atoms in the unit cell. What would happen if we play the game to double, quadruple, etc. the unit cell ?

Figure: (Left) Standard "zone-boundary" Peierls instability (dimerization and unit-cell doubling). (Right) Surface reconstruction of the (very simple) Si(001) surface.

Ideally, a stability study should be completed by a look at the phonon band structure to detect soft modes.

Assessing the merits of DFT in solids: structural properties

Lattice parameters in metals and non-metals

TABLE IV. Statistical data, mean error, mean absolute error, mean relative error (MRE %), and mean absolute relative error (MARE %), for lattice constants (Å) of the 14 metals and 10 nonmetals in the test set of 24 solids calculated with BAND/LCAO from the SJEOS. Comparisons to thermally and ZPAE-corrected experimental results (left) and to partially or uncorrected room temperature experimental values used in Refs. 22 and 41 (right). The best agreement with the experiment are in boldface. For the AM05 values of Table II, compared to corrected experimental results, the total ME and MAE are 0.025 and 0.048 Å, respectively. The AM05 functional performs better for metals (MAE=0.045 Å) than for nonmetals (MAE=0.052 Å).

Solid	Compared to corrected experimental values				Compared to experimental values used in Refs. 22 and 41			
	LDA	PBEsol	PBE	TPSS	LDA	PBEsol	PBE	TPSS
Metals (14)								
ME (Å)	−0.136	**−0.039**	0.046	**0.039**	−0.151	−0.054	**0.030**	**0.024**
MAE (Å)	0.136	**0.042**	0.060	0.060	0.151	**0.058**	0.055	0.060
MRE (%)	−2.71	**−0.76**	0.95	0.74	−3.04	−1.10	**0.61**	**0.39**
MARE[a] (%)	2.71	**0.83**	1.24	1.15	3.04	**1.21**	1.15	1.19
Nonmetals (10)								
ME (Å)	−0.042	**0.026**	0.085	0.066	−0.067	**0.001**	0.060	0.040
MAE (Å)	0.042	**0.026**	0.085	0.066	0.067	**0.001**	0.060	0.043
MRE (%)	−0.86	**0.56**	1.76	1.35	−1.41	**0.00**	1.19	0.79
MARE[a] (%)	0.86	**0.56**	1.76	1.35	1.41	**0.31**	1.19	0.84
Total (24)								
ME (Å)	−0.097	**−0.012**	0.062	0.050	−0.116	**−0.031**	0.043	0.031
MAE (Å)	0.097	**0.036**	0.070	0.062	0.116	**0.040**	0.057	0.053
MRE (%)	−1.94	**−0.21**	1.29	0.99	−2.36	**−0.64**	0.85	**0.56**
MARE[a] (%)	1.94	**0.72**	1.45	1.23	2.36	**0.84**	1.17	1.04

[a](calculated-experimental)/experimental 100%.

Figure: Assessing the performance of recent density functionals for bulk solids, Csonka et al., Phys. Rev. B 79, 155107 (2009). (see Prof. János G. Ángyán in the room)
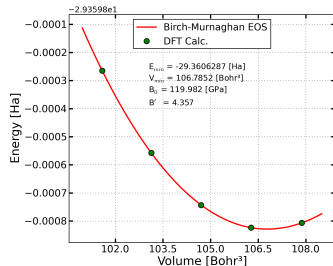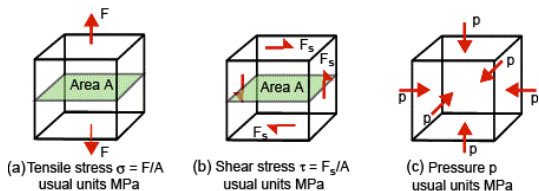
A few words on functionals

There will be this afternoon a lecture on functionals (Pr. Julien Toulouse).

The functional tested in the previous slide are the standard LDA and generalized-gradient approximations (GGA, SOGGA, meta-GGA) of various kinds.

- ▶ LDA usually overbinds (too small interatomic distance or lattice parameter)
- ▶ the original PBE usually underbinds (too large interatomic distance or lattice parameter)
- ▶ the revised PBEsol performs better with no general tendency to over- or under-bind (depends on the system)

Remember however that we are discussing here errors of the order of the percent: this is very remarkable given the "simplicity" of the GGA functionals !! Clearly, it is difficult to find a functional that offers a clear and general improvement for metals and nonmetals.

Other criteria: bulk modulus and cohesive energy

(a) Tensile stress σ = F/A
usual units MPa

(b) Shear stress τ = F_s/A
usual units MPa

(c) Pressure p
usual units MPa

<u>Bulk modulus</u>: $B = \frac{1}{V}\frac{\Delta P}{\Delta V} = \frac{1}{V}\frac{\partial^2 E}{\partial V^2}$. Measure of "stiffness" ($\neq$ hardness).

The <u>cohesive energy</u> is the difference of energy for an atom in the crystal and for the isolated atom. It is an terrible test: a theoretical setup (fonctional, basis, etc.) may be very accurate for the solid, but very bad for the isolated atom (or vice-versa).

Transition metals
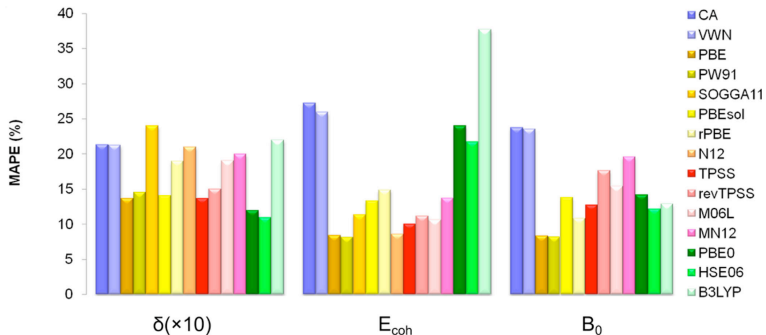
**Figure:** Bulk Properties of Transition Metals: A Challenge for the Design of Universal Density Functionals, Janthon et al, J. Chem. Theory Comput. 2014, 10, 3832.

The introduction of a fraction of exact exchange (hybrid functionals) does not help, and may actually worsen the cohesive energy. Again, the original PBE GGA performs rather well.

Assessing the merits of DFT in solids: electronic properties
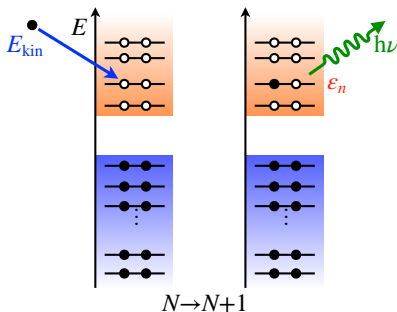
Reminder: direct/inverse photoemission
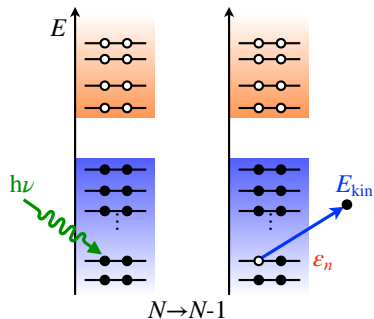
Energy conservation:
$$h\nu + E_0^N = E_{kin} + E_n^{N-1}$$

Identify: $\varepsilon_n = E_0^N - E_n^{N-1}$ $(< \mu)$.

Energy conservation:
$$E_{kin} + E_0^N = h\nu + E_n^{N-1}$$

Identify: $\varepsilon_n = E_n^{N+1} - E_0^N$ $(> \mu)$.

From ΔSCF techniques to the Kohn-Sham equation

A very efficient technique for obtaining the ionization potential and electronic affinity (namely, the HOMO and LUMO frontier orbital energies) in finite size systems is to calculate the total energy of the neutral system and the charged anion and cation. Such a scheme, labeled ΔSCF, mimics the photemission experiment.

This is a real problem in solids: charging one unit cell means charging all units cells periodically $\Rightarrow$ the Coulomb energy diverges !! Further, the ΔSCF technique does not allow to obtain all occupied and unoccupied (virtual) electronic energy levels.

The only thing we are left with is the Kohn-Sham equation:

$$\left(\frac{-\nabla^2}{2} + \hat{V}^{ionic} + \hat{V}^{Hartree} + \hat{V}^{XC} \right) \phi_{n\mathbf{k}}(\mathbf{r}) = \varepsilon_{n\mathbf{k}} \phi_{n\mathbf{k}}(\mathbf{r})$$

The Kohn-Sham equation

In solids, there is one Kohn-Sham equation to be solved for each **k**points in the Brillouin zone. In the planewave formalism, such an equation reads:

$$\sum_{\mathbf{G}'} \left(\frac{(\mathbf{k} + \mathbf{G})^2}{2} \delta_{\mathbf{G},\mathbf{G}'} + V^{eff}(\mathbf{G} - \mathbf{G}') \right) C_{n\mathbf{k}}(\mathbf{G}') = \varepsilon_{n\mathbf{k}} C_{n\mathbf{k}}(\mathbf{G})$$

where the $C_{n\mathbf{k}}(\mathbf{G})$ are the Fourier components of the periodic part $u_{n\mathbf{k}}(\mathbf{r})$ of the Kohn-Sham eigenstate: $\phi_{n\mathbf{k}}(\mathbf{r}) = e^{i\mathbf{k}\cdot\mathbf{r}} u_{n\mathbf{k}}(\mathbf{r})$. The Fourier components of V^{ion}, V^H, and V^{XC} have been discussed above.

Remember however that:

$$E_0 = \sum_{n\mathbf{k}}^{occp} \varepsilon_{n\mathbf{k}} - \frac{1}{2} \int \int \frac{n(\mathbf{r})n(\mathbf{r}')}{|\mathbf{r} - \mathbf{r}'|} + E^{XC} - \int d\mathbf{r}\, n(\mathbf{r}) V^{XC}(\mathbf{r})$$

There is no obvious relation between these $\{\varepsilon_{n\mathbf{k}}\}$ energies and differences of total energy between the neutral and the charged systems.

The Kohn-Sham gap of semiconductors

We compile here below the DFT-LDA Kohn-Sham gap of semiconductors and insulators (red dots; courtesy Valério Olévano) that we compare to the experimental values (first diagonal). We also provide the Hartree-Fock gap (pink dots).
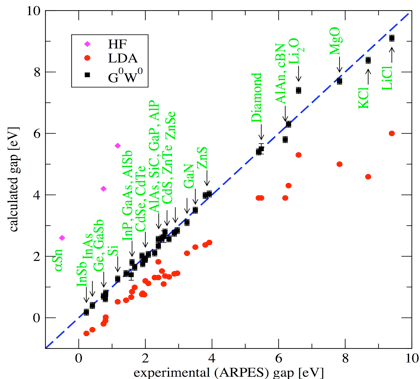
Clearly, the DFT Kohn-Sham gap is too small !! On the contrary, the Hartree-Fock gap is too large. As an important example, the LDA, HF and experimental band gap of silicon are: 0.6 eV, 6.5 eV, and ... 1.2 eV.

The black dots are the results of perturbation theory correcting the Kohn-Sham energies: the *GW* formalism will be the subject of some of next week lectures.

Hartree-Fock theory for the homogeneous electron gas

If we plug in the Hartree-Fock (Roothan) eigenvalue equation:

$$\left(\frac{-\nabla^2}{2} + \hat{V}^{ion} + \hat{V}^H \right) \phi_i(\mathbf{r}) - \sum_j \int d\mathbf{r}' \frac{\phi_j^*(\mathbf{r}')\phi_j(\mathbf{r})\phi_i(\mathbf{r}')}{|\mathbf{r} - \mathbf{r}'|} \delta_{s_i,s_j} = \varepsilon_i \phi_i(\mathbf{r})$$

the only possible form: $e^{i\mathbf{k} \cdot \mathbf{r}} \times |\text{spin} >$ for homogeneous systems, one obtains with the proper $(1/q^2)$ Fourier transform of the Coulomb field:

$$\varepsilon(\mathbf{k}) = \frac{\mathbf{k}^2}{2} - \int_{k' < k_F} \int \frac{d\mathbf{k}'}{(2\pi)^3} \frac{4\pi}{|\mathbf{k} - \mathbf{k}'|^2} = \frac{\mathbf{k}^2}{2} - \frac{2}{\pi} k_F F(k/k_F)$$

with k_F the Fermi wavevector and $F(x) = \frac{1}{2} + \frac{1-x^2}{4x} ln \left| \frac{1+x}{1-x} \right|$.

Such an energy is continuous at the Fermi surface ($k = k_F$) but the slope $\partial \varepsilon(\mathbf{k})/\partial \mathbf{k}$, namely the group velocity, diverges at (k_F).

Short and long range screening in solids

Anticipating on next week *GW* lecture, we will see that nice electronic properties can be obtained with a one-body eigenvalue equation formally resembling the Hartree-Fock equation provided that we use the "screened Coulomb potential" $W(\mathbf{r}, \mathbf{r}')$ rather than the bare Coulomb potential.

When a test charge Q is added to the system at $\mathbf{r}_0$, it will repel/attract locally all surrounding electrons, creating a $\delta n(\mathbf{r})$ variation of the electronic cloud. Within linear response theory (χ the susceptibility):

$$\delta n(\mathbf{r}) = \int d\mathbf{r}' \chi(\mathbf{r}, \mathbf{r}') \frac{Q}{|\mathbf{r} - \mathbf{r}_0|}$$

Fig. 0.11 *Quasi Electron Propagates Through System*

Two Quasi Electrons Interact only Weakly Because of Shielding

The total field generated by Q and $\delta n(\mathbf{r})$ is:

$$W(\mathbf{r}, \mathbf{r}_0) = \frac{Q}{|\mathbf{r} - \mathbf{r}_0|} + \int \frac{d\mathbf{r}' \delta n(\mathbf{r}')}{|\mathbf{r} - \mathbf{r}'|} = V^C(\mathbf{r}, \mathbf{r}_0) + \int d\mathbf{r}' d\mathbf{r}'' V^C(\mathbf{r}, \mathbf{r}') \chi(\mathbf{r}', \mathbf{r}'') V^C(\mathbf{r}'', \mathbf{r}_0)$$
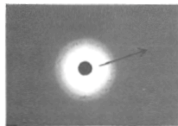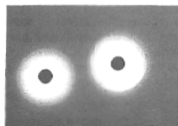
Short and long range screening in solids (II)

Introduce the dielectric function (ϵ) as: $W(\mathbf{r}, \mathbf{r}') = \int d\mathbf{r}'' \epsilon^{-1}(\mathbf{r}, \mathbf{r}'') V^C(\mathbf{r}, \mathbf{r}'')$.
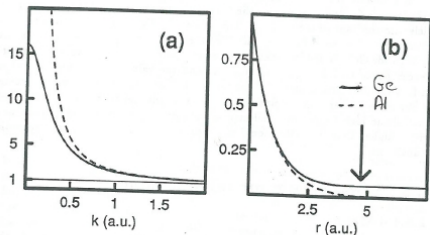

Figure 2.1. (a): Diagonal dielectric functions $\epsilon(k)$ for Al (dashed) and Ge (solid) (b): Ratio $\phi(r)/\phi_0(r)$ between the screened and unscreened potentials of a point charge, from the dielectric functions shown in (a).

Figure courtesy Rafaelle Resta, SISSA lecture notes.

In a metal (dotted line), the screened Coulomb potential is short-ranged: it is usually described by a Yukawa-like potential: $e^{-k_F r}/r$.

In semiconductors, screening is imperfect and the long-range behavior of the screened Coulomb potential is: $1/(\epsilon_M r)$ where ϵ_M is the macroscopic dielectric constant (e.g. ϵ_M=11.9 for silicon, ϵ_M=5.3 for diamond).

Hybrid functionals and the dielectric constant

The previous slide tells us that in metals long-range bare exchange in metals is somehow inappropriate. Global hybrids such as PBE0 or B3LYP may not be the ideal choice and one should favor a short-range version of the exchange functional using e.g. the following decomposition of the Coulomb potential.

$$\frac{1}{|\mathbf{r} - \mathbf{r'}|} = \frac{erf(\omega|\mathbf{r} - \mathbf{r'}|)}{|\mathbf{r} - \mathbf{r'}|} \quad \text{(long range)}$$

$$+ \frac{erfc(\omega|\mathbf{r} - \mathbf{r'}|)}{|\mathbf{r} - \mathbf{r'}|} \quad \text{(short range)}$$
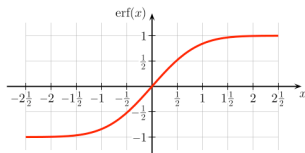
In semiconductors, a strategy could be to keep precisely a fraction of long range exchange governed by $1/\epsilon_M$. This can be more formally derived from perturbation theory, yielding the so-called screened-exchange term:

$$\Sigma_{SEX} \simeq \frac{-1}{\epsilon_M} \sum_n^{occp} \frac{\phi_n(\mathbf{r})\phi_n^*(\mathbf{r'})}{|\mathbf{r} - \mathbf{r'}|}$$

Hybrid functionals from ϵ_M in semiconductors

|		PBE	PBE0	hybrid	hybrid	sc-hybrid	Exp.
	Type	$\alpha=0$	$\alpha=0.25$	$\alpha=1/\epsilon_\infty^{PBE}$	$\alpha=1/\epsilon_\infty^{PBE0}$	$\alpha=1/sc\text{-}\epsilon_\infty$	
Ge	(dC)	0.00	1.53	–	0.77	0.71	0.74[84]
Si	(dC)	0.62	1.75	0.96	1.03	0.99	1.17[84]
AlP	(ZB)	1.64	2.98	2.31	2.41	2.37	2.51[85]
SiC	(ZB)	1.37	2.91	2.23	2.33	2.29	2.39[86]
TiO$_2$	(Ru)	1.81	3.92	2.83	3.18	3.05	3.3[87]
NiO	(RS)	0.97	5.28	2.00	4.61	4.11	4.3[88]
C	(dC)	4.15	5.95	5.37	5.44	5.42	5.48[89]
CoO	(RS)	0.00	4.53	–	4.01	3.62	2.5[90]
GaN	(ZB)	1.88	3.68	3.10	3.30	3.26	3.29[91]
ZnS	(ZB)	2.36	4.18	3.65	3.85	3.82	3.91[84]
MnO	(RS)	1.12	3.87	2.55	3.66	3.60	3.9[92]
WO$_3$	(M)	1.92	3.79	3.24	3.50	3.47	3.38[93]
BN	(ZB)	4.49	6.51	6.24	6.34	6.33	6.25[94a]
HfO$_2$	(M)	4.32	6.65	6.38	6.68	6.68	5.84[95]
AlN	(WZ)	4.33	6.31	6.07	6.24	6.23	6.28[96]
ZnO	(WZ)	1.07	3.41	3.06	3.73	3.78	3.44[97]
Al$_2$O$_3$	(Cr)	6.31	8.84	9.42	9.65	9.71	8.8[98]
MgO	(RS)	4.80	7.25	7.97	8.24	8.33	7.83[99]
LiCl	(RS)	6.54	8.66	9.42	9.57	9.62	9.4[100]
NaCl	(RS)	5.18	7.26	8.55	8.73	8.84	8.6[101]
LiF	(RS)	9.21	12.28	15.48	15.83	16.15	14.2[102]
H$_2$O	(XI)	5.57	8.05	11.19	11.44	11.71	10.9[103]
Ar	(cF)	8.78	11.20	14.40	14.54	14.67	14.2[104]
Ne	(cF)	11.65	15.20	23.32	22.99	23.67	21.7[104]
ME (eV)		-2.7	-0.3	0.0	0.3	0.3	–
MAE (eV)		2.67	1.08	0.5	0.4	0.5	–
MRE (%)		-46.9	10.8	-1.1	4.9	3.3	–
MARE (%)		46.9	21.1	9.6	7.4	7.8	–

In semiconductors, the use of global hybrids with the percentage α of non-local exchange (v_x^{ex}) governed by $1/\epsilon_M$:

$$v_{xc}(\mathbf{r}, \mathbf{r}') = \alpha v_x^{ex}(\mathbf{r}, \mathbf{r}') + (1 - \alpha)v_x(\mathbf{r})$$
$$+ v_c(\mathbf{r}), \quad \text{with:} \quad \alpha = 1/\epsilon_M$$

was shown to produce much better band gaps in insulators and semiconductors (Figure from Skone et al. PRB 89, 195112 (2014); see also: Marques et al. PRB 83, 035119 (2011)).

Complement: 0D, 1D, 2D systems with periodic boundary conditions

(Figure courtesy Xavier Gonze)

Molecule

Surface : treatment of a slab

Point defect in a bulk solid
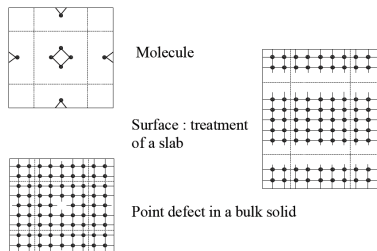
If the molecule, surface, etc. has a permanent dipole, quadrupole, ... the cell-cell interaction is long-range: corrective terms must be added to cancel these slowly vanishing interactions (Markov/Payne, 95).

Codes with periodic boundary conditions can be used to study 0D, 1D, 2D systems: the price to pay is to introduce sufficient vacuum to avoid cell-cell interactions.

Remember that with planewaves, the size of the basis for a given energy cutoff is proportional to the unit cell volume:

$\Omega_{BZ} = (2\pi)^3/\Omega_{cell} \Rightarrow$ basis size=

$N_G = \frac{4}{3}\pi G_{max}^3/\Omega_{BZ} \simeq \Omega_{cell}$

One has to pay for the vacuum !
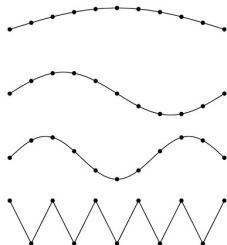
Density functional perturbative theory (DFPT)

Let's take the example of the phonons, namely the vibrational modes. The standard approach is to build the dynamical matrix and find its eigenvectors:

$$det \left| \frac{1}{\sqrt{M_I M_J}} \frac{\partial^2 E(\{\mathbf{R}\})}{\partial \mathbf{R}_I \partial \mathbf{R}_J} - \omega^2 \right| = 0$$

It is certainly easy to calculate the change in energy by changing the position of the atoms in the unit cell. But if the wavelength of the phonon mode becomes very large, then the unit cell to consider becomes ... extremely large.
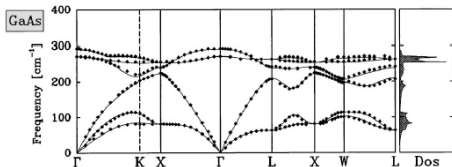
GaAs phonon band structure (LDA and experiment: Baroni et al. Rev. Mod. Phys. 2001).

Density functional perturbative theory (DFPT)

To calculate phonon modes with very large wavelength (small $\mathbf{q}$), or a wavelength incommensurate with the lattice periodicity, the solution is perturbation theory where you work with the zeroth-order (unperturbed) eigenstates (ε_n, ϕ_n):

$$(\hat{H}_{SCF} - \varepsilon_n)|\delta\phi_n\rangle = (\delta V^{SCF} - \delta\varepsilon_n)|\phi_n\rangle \quad \text{with:} \quad \delta V^{SCF} = \delta V^{ion} + \delta V^{HXC}$$

and: $\delta n(\mathbf{r}) = \sum_n^{occp} \phi_n^*(\mathbf{r})\delta\phi_n(\mathbf{r}) + cc = \sum_{m \neq n} \phi_n^*(\mathbf{r})\phi_m(\mathbf{r})\frac{\langle\phi_m|\delta V^{SCF}|\phi_n\rangle}{\varepsilon_n - \varepsilon_m} + cc$

There are however two problems:

- how do we calculate $\langle\phi_m|\delta V^{SCF}|\phi_n\rangle$ (e.g. δV^{SCF} incommensurate) ?
- we need all the solutions of the Kohn-Sham Hamiltonian: too expensive in general.

First-order perturbation theory

In the expression for $\delta n(\mathbf{r})$, terms where both (n,m) refer to occupied (unoccupied) states cancel each other. As such, δn is built out of matrix elements coupling only occupied (v=valence) and unoccupied (c=conduction) states. With $\hat{P}_c$ the projector over the unoccupied state manifold:

$$\hat{P}_c(\hat{H}_{SCF} - \varepsilon_n)|\delta\phi_v\rangle = \hat{P}_c(\delta V^{SCF} - \delta\varepsilon)|\phi_v\rangle$$

$$\Rightarrow (\hat{H}_{SCF} - \varepsilon_n)\hat{P}_c|\delta\phi_v\rangle = \hat{P}_c\delta V^{SCF}|\phi_v\rangle$$

Writing $|\delta\psi_v\rangle = \hat{P}_c|\delta\phi_v\rangle$ and $\hat{P}_c = 1 - \hat{P}_v$, with: $\hat{P}_v = \sum_v |\phi_v\rangle\langle\phi_v|$ is the projector on the occupied levels, we have:

$$(\hat{H}_{SCF} - \varepsilon_n)|\delta\psi_v\rangle = (1 - \hat{P}_v)\delta V^{SCF}|\phi_v\rangle \quad \text{with:} \quad \delta V^{SCF}(\mathbf{r}) = \delta V^{ion}(\mathbf{r}) + \delta V^{HXC}[n]$$

$$\delta n(\mathbf{r}) = \sum_v \phi_v^*(\mathbf{r})\delta\psi_v(\mathbf{r}) + cc$$

This is just a simple self-consistent scheme to be solved for the $(\delta\psi_v)$.

First-order perturbation theory

Putting back the **k**-point, we still need to calculate : $\langle \phi_{v'\mathbf{k}'}|\delta V^{SCF}|\phi_{v\mathbf{k}}\rangle$, where δV^{SCF} can be incommensurate with the lattice periodicity.

Assume a monochromatic perturbation $\delta V_{\mathbf{q}}^{ion}$ of momentum (**q**). Due to periodicity, the only nonzero matrix elements are such that: $\mathbf{k}' = \mathbf{k} + \mathbf{q}$.

$$\langle \phi_{v'(\mathbf{k}+\mathbf{q})}|\delta V^{SCF}|\phi_{v\mathbf{k}}\rangle$$
$$= \langle u_{v'(\mathbf{k}+\mathbf{q})}|\delta w_{\mathbf{q}}^{SCF}|u_{v\mathbf{k}}\rangle,$$

where the (u) and (w) are the periodic part of the Bloch ϕ and δV^{SCF} electronic and perturbation Bloch waves. Such matrix elements can be easily calculated in Fourier components.
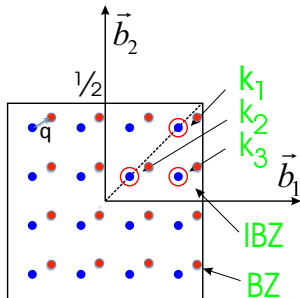

Figure: double **k**- and (**k** + **q**)-point grid needed to calculate the perturbation matrix elements.

Complement: The ionic energy and Ewald summations

This term is not specific to planewave formulations, but the Ewald summation "technology" is an important aspect of codes. The summation of the Coulomb interaction between point charges converges very slowly both in real-space ($1/R$ behaviour) and in reciprocal-space ($1/G^2$ behaviour). The trick is to use Ewald's summation technique, adding/subtracting a Gaussian charge:

$$Q_J = Q_J \left(1 - \left(\frac{\alpha}{\pi} \right)^{3/2} e^{-\alpha(\mathbf{r} - \tau_J)^2} \right) + Q_J \left(\frac{\alpha}{\pi} \right)^{3/2} \exp(-\alpha(\mathbf{r} - \tau_J)^2)$$

with $(Q_J = eZ_J, \tau_J)$ the charge and position of the ion (J).

Original   Direct   Reciprocal
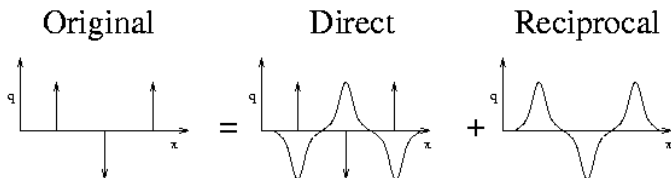
The field created by a Gaussian charge is the Coulomb field attenuated by a complementary error function: the sum converges quickly in real space !

Complement: The pseudoptential approximation (II)

"Norm-conserving" pseudopotentials: $\int_{r<r_c} dr |\phi_{ps}(r)|^2 = \int_{r<r_c} dr |\phi_{ae}(r)|^2$
improves the "transferability" (see the $(d/d\varepsilon)$ in the following relation):

$$-2\pi \left[(r\phi(r))^2 \frac{d}{d\varepsilon} \left(\frac{d}{dr} ln\phi(r) \right) \right]_{r_c} = 4\pi \int_0^{r_c} dr |\phi(r)|^2$$

Continuity of the wavefunction and its derivative is enforced for smoothness.

The pseudopotentials are non-local: each (lm)-channel sees its own pseudopotential (with non-negligible consequences on the standard $[x, p_x]$ commutators). The Kleinman-Bylander transformation leads to a "separable form" for the non-local part (less "ghost-states" and more efficient):

$$V^{ps}(\vec{r}) = V^{loc}(r) + \sum_{ml} v_l |\beta_{lm}\rangle\langle\beta_{lm}|$$

V^{loc} as a (-Z/r) tail and the nonlocal parts (projectors) are short-ranged.

References: Haman et al. Phys. Rev. Lett. 43, 1494 (1979); Kleinman et al. Phys. Rev. Lett. 48, 1425 (1982); Gonze et al. Phys. Rev. B 44, 8503 (1991).